Int J Earth Sci (Geol Rundsch) (2014) 103:597–602
DOI 10.1007/s00531-013-0973-6

SHORT NOTE

Kinematics of horizontal simple shear zones of concentric arcs (Taylor–Couette flow) with incompressible Newtonian rheology

Soumyajit Mukherjee · Rakesh Biswas

Received: 11 March 2013 / Accepted: 22 October 2013 / Published online: 15 November 2013

Abstract We present preliminary kinematic analyses of Taylor–Couette flow. We consider deformation of a Newtonian incompressible ductile material inside rotating horizontal listric (concentric circular) boundaries. The velocity profile is curved indicating non-uniform shear strain but leads to the same shear sense. Each material point on progressive shear keeps increasing shear strain linearly with time. A curve of no movement, the 'neutral curve', may exist inside the shear zone. Irregular geometries of initially regular markers and their individual non-matching strain paths indicate inhomogeneous deformaion in such Taylor–Couette flow.

Keywords Simple shear · Shear zone · Shear sense · Couette flow · Inhomogeneous deformation · Newtonian fluid

Introduction

Shear zones are 'tabular or sheetlike, planar or curviplanar zones in which rocks are more highly strained than rocks adjacent to the zone' (Davis et al. 2012). Understanding shear zone kinematics is important in tectonics since the major plate boundaries are defined by such zones (Regenauer-Lieb and Yuen 2003), and extrusion and subduction might be shear controlled (e.g. Beaumont et al. 2001; Stüwe 2007). Recently Mukherjee (2012) reinterpreted kinematics of simple shear zones with parallel and inclined boundaries and demonstrated development of non-uniform shear senses.

However, shear zones that were assumed simplistically to have parallel straight boundaries, e.g. the Main Central Thrust and the South Tibetan Detachment System that bound the Higher Himalaya, were found later to be curves in macro-scales based on several geophysical studies (e.g. fig. 1 of Beaumont et al. 2001 and references therein). Such listric geometry of faults develops probably because the fault plane passes from a brittle regime at surface into a ductile regime at depth. Exposures of the boundaries of the orogen-scale shear zones are more commonly curved than straight (e.g. Xypolias and Doutsos 2000; Lin and Jiang 2001; Xypolias and Kokkalas 2006). Regional reverse shear (thrust) planes that translate nappes are curved, and at places give normal shear sense (Merle 1998). Curved primary ductile shear planes have been known since 1970s in meso-scales (e.g. Coward 1976) and subsequently in hand-specimen scales (figs. 2e and 7b of Gapais et al. 1987). Also, stressed hypoplastic granular media may develop curved fault planes (e.g. Tejchman 2008). Shear zones of high strain have been mentioned to have curved boundaries, where simple shear prevailed (Simpson and De Paor 1993; also see Coward 1976). Coward (1976) further mentioned that shear zones that either 'grew' slowly or were blocked at one side can curve their boundaries. He considered anastomosed foliations, what also are described as 'step-overs' or 'over-steps' (latest review and original reports in Mukherjee 2013a), inside shear zones as (an indirect) field evidence of their curved boundaries. Brun and Burg (1982) stated that curved shear zones can develop in collisional tectonic settings where corner flow exists. Curved boundaries of the Greater Himalayan Crystallines, viz. the Main Central Thrust at S/SW and the South Tibetan Detachment Zone at N/NE, are 6–50 km away in different

S. Mukherjee (✉) · R. Biswas
Department of Earth Sciences, Indian Institute of Technology Bombay, Powai, Mumbai 400 076, Maharashtra, India
e-mail: soumyajitm@gmail.com

rivers sections (reviews by Mukherjee and Koyi 2010a, b; Mukherjee 2013b). On the other hand, for the sake of simplicity, structural geological texts so far presented shear zones to be bound by straight boundaries (e.g. Ramsay 1980; Ramsay and Lisle 2000).

Only a few attempted to deduce the kinematics of shear zones in other cases, such as with non-parallel straight boundaries under simple shear (e.g. Mandal et al. 2002), and Poiseuille flow (e.g. Mukherjee et al. 2012). Even though deformation behaviour around particles inside curved shear zones were analogue modelled (e.g. Exner et al. 2006), kinematics of these ductile shear zones did not receive any focus by other geologists. This is despite the fact that flow between concentric rotating cylinders has long been discussed in fluid mechanics as 'Taylor–Couette flow', 'circular shear', 'circular Couette flow', etc. (Donnelly 1991; Schlichting and Gersten 1999).

This work presents an analytical model of simple shear of a zone bound by concentric circular arcs. Although shear fabrics decode only the relative shear sense (Passchier and Trouw 2005; Mukherjee 2011, 2013c, d), this work follows Mukherjee (2012) to consider absolute movement of the shear zone boundaries.

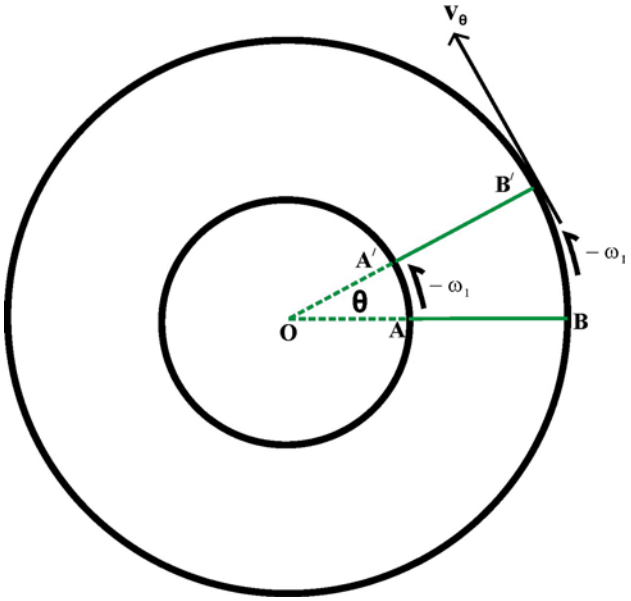

Fig. 1 An angular velocity of $-\omega_1$ acts on the two concentric circles. An undeformed straight marker AB on shear attains A′B′ at a particular instant. Azimuthal velocity (v_θ) and meridional angle (θ) are defined inside the figure

The model

A curved ductile shear zone consisting of two horizontal concentric rigid circular arcs as its boundaries is considered to be full of a Newtonian viscous fluid. In this case, the vorticity vector (fig. 1 of Passchier and Coelho 2006) is vertical. An incompressible fluid with no kinematic dilatancy is considered. We ignore viscous dissipation (such as Mukherjee and Mulchrone 2013) and radioactive heating leading to any change in viscosity and/or density, any pure shear component and its temporal variation, widening/narrowing of the shear zone, deformation of the boundaries, why the shear zone is curved and how/whether it propagates spatially, heterogeneity in composition, pressure gradient, (partial) melting, metamorphism, evolution of (micro)structures such as folds, strain partitioning, non-Newtonian behaviour such as shear thickening/thinning, etc. Being a horizontal shear zone, its deformation remains unaffected by the acceleration due to gravity ('g'), geothermal gradient and any change in density and/or viscosity dependent to temperature and depth. This is similar to some of the previous models of shear zones (e.g. Ramsay 1980; Ramsay and Lisle 2000; Grasemann et al. 2006; Mukherjee 2012 etc.).

If the two boundaries rotate at same rate and at the same direction, no 'shear' develops (Eq. 1 in Appendix). The velocity profile in this case is a straight line that passes through the centre of the two concentric boundaries

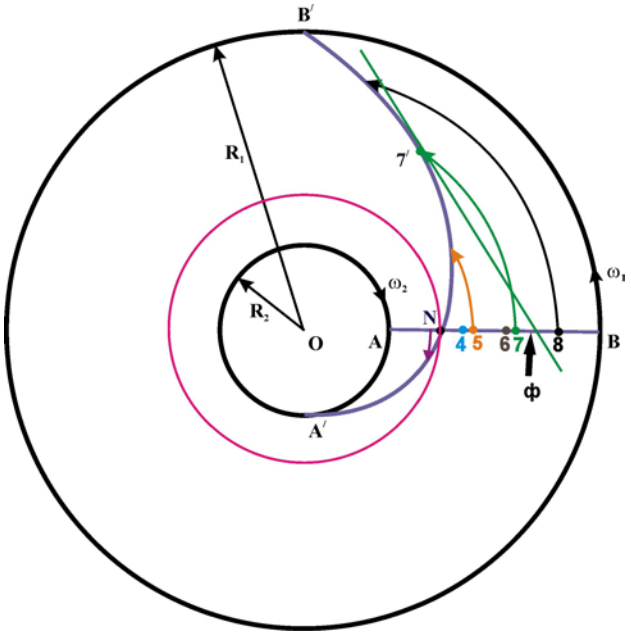

Fig. 2 Two concentric circular margins of radii R_1 and R_2 ($R_1 > R_2$) bound a ductile shear zone. Rotation of the outer boundary with an anticlockwise angular velocity $-\omega_1$ and the inner one with a clockwise ω_2 creates a velocity profile A′B′. AB was the undeformed marker before deformation started. Intersection between A′B′and AB defines the *neutral point* 'N'. The red circle passing through N is the *neutral curve*. *Full arrows* show the curvilinear flow paths of points *5*, *6* and *8*. Here: $R_1 = 100$ cm, $R_2 = 50$ cm, $\omega_1 = \omega_2 = 2°\ s^{-1}$. Angular shear strain ($\phi$) at point '7′': angle between a tangent on the profile drawn at that point and the line AB

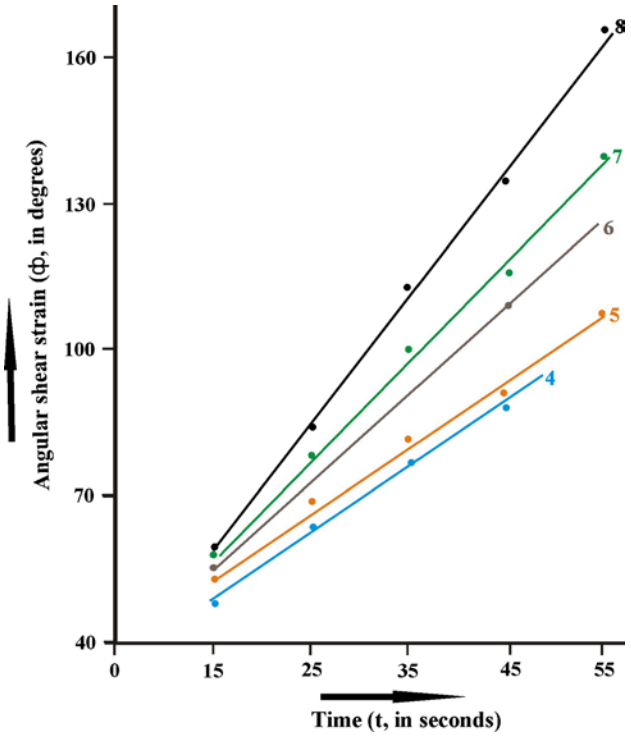

Fig. 3 Variation of angular shear strain (ϕ) with time (t) for points 4, 5, 6, 7 and 8 as shown in Fig. 2

(Fig. 1). However, when the boundaries rotate with (1) different rates (=angular velocities) in the same direction, (2) different rates in opposite direction, (3) same rate but in opposite direction, and (4) one of the boundaries rotate and the other remain stationary, 'shear' develops and the velocity profile is curved (Fig. 2). Points on the undeformed marker line keep increasing angular shear strain (ϕ) linearly with time (Fig. 3). ϕ at any instant is the angle between the lines before and after deformation. As per Fig. 3, a point '7' was initially on line AB and is now as '7′', and ϕ is the angle between AB and the tangent on the profile at '7′'. Inside the shear zone, a gradient in shear strain develops. For example, in Fig. 3, at $t = 35$ s, markers 4–8 show progressive increase in shear strain. In very slow slip rate of the boundaries of the order of a few mm per year as expected in natural shear zones, flow paths will be curved lines parallel to the shear zone boundaries (e.g. Fig. 2). Unlike curved velocity profiles generated usually in inclined simple shear zones with straight parallel boundaries (e.g. fig. 1b of Mukherjee 2012), the shear sense in the present case does *not* flip. As expected, this is in fact similar to horizontal simple shear zones with straight boundaries where uniform shear sense is produced. The only significant difference remains that while in the present model, and angular shear strain varies from point to point on the curved velocity profile; a uniform shear strain is produced in simple shear zones with horizontal straight boundaries. Thus, curvature of the boundaries of the shear zone can impart significant deviation in shear strain and develop a different kinematics. In the present case of curved horizontal shear zone, the velocity profile depends on (1) the angular velocities and (2) the radii of the two boundaries (Eq. 4 in Appendix). It is thus independent of viscosity and density of the shear zone material.

When the two boundaries of the shear zone slip oppositely, the resultant velocity profile intersects the initial position of that line in undeformed state at a point (Fig. 2). This point is the 'neutral point'. Its coordination is presented in the Appendix after Eq. (4). A circle passing through this point and concentric to the shear zone boundaries defines a 'neutral curve' of no movement during ductile shear. Without mentioning its significance much, Lister and Williams (1983) described the neutral curve in simple shear zones with parallel boundaries as a straight line and called it the 'plane of shear'. However, shear strains on points lying on neutral curve are *not* zero. Even if the two boundaries shear with the same magnitude of angular velocity but in opposite directions, the neutral point does *not* plot at the middle of the circular shear zone (as in Fig. 2). This mismatches with what Mukherjee (2012) showed for horizontal simple shear zone with parallel boundaries. The reason is that while in the second case, the velocity profile is straight, and in the present model, it is a curved line. If the two boundaries of the shear zone slip in the same direction, the neutral point lies outside the shear zone. The neutral point in this case is located by extrapolating both the velocity profile and the undeformed marker line before shear initiated. In other words, in such cases, all points inside the shear zone undergo slip and movement. Neutral point exists in simple shear zones with parallel boundaries. However, in that case, the neutral curve is a straight line (e.g. Mukherjee 2012; Mukherjee and Mulchrone 2013). Deviation in angular velocities (=slip rates) of the boundaries obviously relocates the neutral point.

Deformations of several circular markers inside the circular shear zone show that unlike simple shear zones with straight boundaries, the markers do *not* turn elliptical (Fig. 4). Their irregular shapes indicate that the studied deformation pattern is in fact inhomogeneous. Even if we had taken smaller markers, those would have deformed inhomogeneously. At any particular instant, different markers attain different irregular shapes. The markers deform in such a manner that relative rotation direction of the outer boundary of the shear zone is from the convex sides of the deformed markers towards their concave sides. This can be understood from Fig. 4 by comparing the direction of rotation of the outer boundary and the geometries of the deformed markers. The exact geometries of individual strain ellipses will depend also on the radii of the two

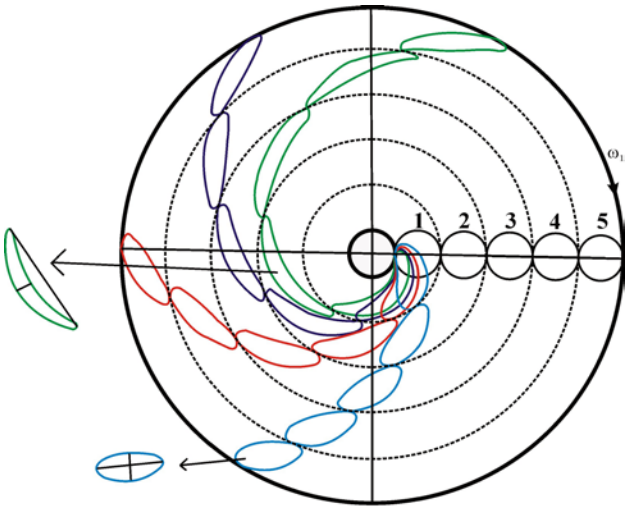

Fig. 4 A circular shear flow when only the outer boundary rotates and the inner boundary is stationary. Five circular markers undergo inhomogeneous deformation and produce irregular geometries—shown in four instances. Here, the outer circular boundary is considered to have a radius of 100 cm and the inner one of 50 cm. Also considered are: $\omega_1 = 2^\circ\ s^{-1}$; *blue markers* after 60 s; *red markers* after 90 s; *violet markers* after 120 s; *green markers* after 150 s

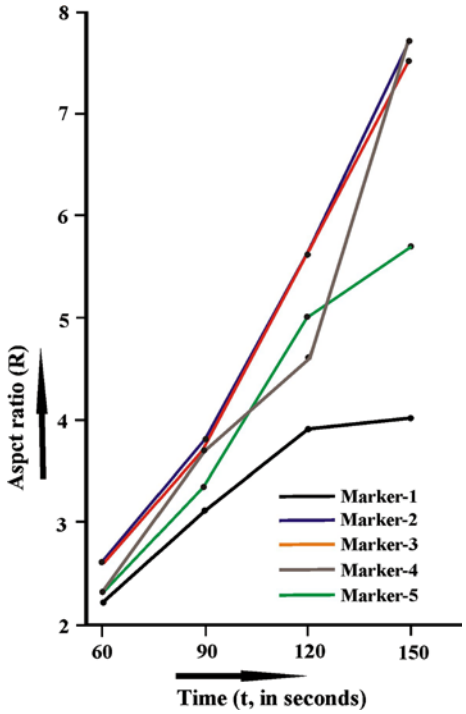

Fig. 5 Aspect ratios (R) versus time (t) variations for the five markers, as in Fig. 4, are plotted

circular arcs as well as that of the circular markers. A plot of aspect ratios (R) of the deformed markers versus time (t) shows that R in general increases temporally (Fig. 5). Aspect ratio (R) in this study is defined as: R = length of the line (PQ) joining the farthest points on the markers divided by the maximum thickness of the marker perpendicular to PQ. The parameters in the numerator and the denominator are shown for deformed markers in two cases in Fig. 4. Interestingly, the R-t paths for these markers are 'non-parallel' (or are 'different'). This is expected in an inhomogeneous deformation. In contrast, horizontal simple shear zones with straight parallel boundaries give parallel (or same) strain paths for different circular markers indicating they attain the same strain at any particular instant.

For inclined shear zones with parallel boundaries, the velocity profile depends additionally on the dip of the shear zone, and the viscosity and the density of the rock material (e.g. Mukherjee 2012). These parameters appear since a component of weight of the shear zone material acts along its down-dip direction. Since we considered horizontal shear zones, these parameters did not come into the velocity profile, i.e. Eq. 4 in Appendix. A component of pressure gradient sometimes act in inclined shear zones either to subduct (e.g. Stüwe 2007) or to extrude (e.g. Beaumont et al. 2001) rocks by Poiseuille flow mechanism (Schlichting and Gersten 1999). Since we considered horizontal shear zones that neither subducts nor extrudes, no pressure gradient component was considered.

Natural curved shear zone may not have perfectly circular boundaries. In those cases, the velocity profile and therefore the location of the neutral point would vary. However, in absence of models with curved boundaries same as the natural prototypes, this work cannot specify the extent of this modification.

Conclusions

Ductile shear zones in depth are usually curved. As a first step to understand their kinematics, we assume that these zones are incompressible Newtonian viscous and bound by concentric rigid circular arcs. For the sake of simplicity, listric horizontal shear zones were considered. This is practically same as the well known Taylor–Couette flow in fluid mechanics. The velocity profiles of simple shear in such cases are functions of the radii of the two circular boundaries and their rates of slip (=rotation). Even though the profile is not a straight line, the sense of shear inside the shear zone remains uniform, and the angular shear strain at different points on the marker line increases linearly with time. The point that remains stationary on the velocity profile, either inside the shear zone, or outside when the profile is extrapolated, is called the 'neutral point'. A line passing through this point and parallel to the curved boundary defined a 'neutral curve' of no

movement. Had we considered circular shear zone to be inclined, the velocity profile would presumably dependent on density and viscosity of the shear zone material as well.

The new points coming out of this work are (1) shear strain at any particular time instant at different points on the deformed marker is unequal, (2) deformation in circular shear zone is inhomogeneous where the aspect ratios of markers keeps increasing in a non-uniform manner and (3) curvature of shear zone boundaries significantly controls the velocity profiles and the location of the neutral point. However, for gently curved boundaries, almost linear velocity profile would be expected. The present model applies theoretically to curved shear zones of any arc length.

Acknowledgments This work is a part of RB's M.Tech. dissertation funded by IIT Bombay. Department of Science and Technology's (New Delhi) grant: IR/S4/ESF-16/2009(G) supported SM. Paris Xypolias (University of Patras) and Paul Bons (University of Tuebingen) are thanked for positive critical reviews. The authors thank Christian Dullo (IFM Geomar) for Chief Editorial handling, his wife Monika Dullo for managerial editorial works, and the Associate Editor Karel Schulman. Shirley Paul and Citra Namperumal are thanked for proofreading.

Appendix

Fluid motion in the annulus between two rotating concentric cylinder is (eqn 15.38 of Williams and Elder 1989):

$$0 = [d^2 v_\theta / dr^2 + d/dr(v_\theta / r)] \tag{1}$$

Here, v_θ: linear velocity of fluid along the azimuthal direction; θ: meridional angle (defined in Fig. 1); r: distance between the centre and the spot where the velocity (v_θ) is considered.

Integrating Eq. (1) twice:

$$v_\theta = C_1 r / 2 + C_2 / r \tag{2}$$

Here, C_1 and C_2 are integration constants.

When both the boundaries rotate in the same direction with the same speed, i.e. at both $r = R_1, R_2$; $v_\theta = -R_1\omega_1$, the velocity profile becomes:

$$v_\theta = -\omega_1 \tag{3}$$

When the outer boundary rotates anticlockwise with an angular velocity $-\omega_1$ and the inner one clockwise with ω_2, i.e. at $r = R_1$, $v_\theta = -R_1\omega_1$; and at $r = R_2$, $v_\theta = R_2\omega_2$, the velocity profile (Fig. 2) is given by:

$$v_\theta = \left[\left\{(\omega_1 + \omega_2).R_1^2 R_2^2\right\} \Big/ \left(R_1^2 - R_2^2\right)\right] r^{-1} - \left[\left(R_1^2\omega_1 + R_2^2\omega_2\right) \Big/ \left(R_1^2 - R_2^2\right)\right] r \tag{4}$$

In Eq. (3), putting $v_\theta = 0$, and solving r, we obtain the *polar coordinate* of the 'neutral point':

$$\left[\pm R_1 R_2 \left\{(\omega_1 + \omega_2) / \left(R_1^2\omega_1 + R_2^2\omega_2\right)\right\}^{1/2}, 0\right]$$

One of these coordinates falls inside the shear zone, and the other outside it.

When only the outer boundary is static ($\omega_1 = 0$; $\omega_2 \neq 0$), one of the neutral points $(0, R_1)$ lies on the outer boundary of the shear zone. Similarly, when only the inner boundary is static ($\omega_2 = 0$; $\omega_1 \neq 0$), one of the neutral points $(0, R_2)$ lies on the outer boundary.

At least one of the neutral points lies inside the shear zone if the two boundaries rotate in opposite directions (i.e. if $\omega_1 > 0$ then $\omega_2 < 0$ and vice versa) (Fig. 2). Both the neutral points plot outside the shear zone if both the boundaries rotate in the same direction but with unequal speed (i.e. either $\omega_1 \neq \omega_2 > 0$ or $\omega_1 \neq \omega_2 < 0$).

References

Beaumont C, Jamieson RA, Nguyen MH et al (2001) Himalayan tectonics explained by extrusion of a low-viscosity crustal channel coupled to focused surface denudation. Nature 414:738–742

Brun J-P, Burg J-P (1982) Combined thrusting and wrenching in the Ibero-Armorican arc: a corner effect during continental collision. Earth Planet Sci Lett 61:319–332

Coward MP (1976) Strain within ductile shear zones. Tectonophysics 34:181–197

Davis GH, Reynolds SJ, Kluth CF (2012) Structural geology of rocks and regions, 3rd edn. Wiley, Hoboken, NJ

Donnelly RJ (1991) Taylor–Couette flow: the early days. Phys Today 44:32–39

Exner U, Grasemann B, Mancktelow NS (2006) Multiple faults in ductile simple shear: analog modeling of flanking structure systems. In: Buiter SJH, Schreurs G (Eds) Analogue and numerical modeling of crustal-scale processes. Geol Soc Lond 253:381–395 (Spec Publ)

Gapais D, Bale P, Choukroune P et al (1987) Bulk kinematics from shear zone flattening: some field examples. J Struct Geol 9:635–646

Grasemann B, Edwards MA, Wiesmayr G (2006) Kinematic dilatancy effects on orogenic extrusion. In: Law RD, Searle MP, Godin L (eds) Channel flow, ductile extrusion and exhumation in continental collisional zones, vol 268. Geological Society of London, Special Publication, pp 183–199

Lin S, Jiang D (2001) Using along-strike variation in strain and kinematics to define the movement direction of curved transpressional shear zones: an example from northwestern Superior Province, Manitoba. Geology 29:767–770

Lister GS, Williams PF (1983) The partitioning of deformation in flowing rock masses. Tectonophysics 92:1–33

Mandal N, Samanta S, Chakraborty C (2002) Flow and strain patterns at the terminations of tapered shear zones. J Struct Geol 24:297–309

Merle O (1998) Emplacement mechanisms of nappes and thrust sheets. Kluwer, Dordrecht

Mukherjee S (2011) Mineral fish: their morphological classification, usefulness as shear sense indicators and genesis. Int J Earth Sci 100:1303–1314

Mukherjee S (2012) Simple shear is not so simple! Kinematics and shear senses of Newtonian viscous simple shear zones. Geol Mag 149:819–826

Mukherjee S (2013a) Higher Himalaya in the Bhagirathi section (NW Himalaya, India): its structures, backthrusts and extrusion mechanism by both channel flow and critical taper mechanisms. Int J Earth Sci 102:1851–1870

Mukherjee S (2013b) Channel flow extrusion model to constrain dynamic viscosity and Prandtl number of the Higher Himalayan Shear Zone. Int J Earth Sci 102:1811–1835

Mukherjee S (2013c) Deformation microstructures in rocks. Springer, Heidelberg, pp 1–111

Mukherjee S (2013d) Atlas of shear zone structures in Meso-scale. Springer, Heidelberg

Mukherjee S, Koyi HA (2010a) Higher Himalayan Shear Zone, Sutlej section: structural geology and extrusion mechanism by various combinations of simple shear, pure shear and channel flow in shifting modes. Int J Earth Sci 99:1267–1303

Mukherjee S, Koyi HA (2010b) Higher Himalayan Shear Zone, Zanskar Indian Himalaya: microstructural studies and extrusion mechanism by a combination of simple shear and channel flow. Int J Earth Sci 99:1083–1110

Mukherjee S, Mulchrone KF (2013) Viscous dissipation pattern in incompressible Newtonian simple shear zones: an analytical model. Int J Earth Sci 102:1165–1170

Mukherjee S, Koyi HA, Talbot CJ (2012) Implications of channel flow analogue models for extrusion of the Higher Himalayan Shear Zone with special reference to the out-of sequence thrusting. Int J Earth Sci 101:253–272

Passchier C, Coelho S (2006) An outline of shear-sense analysis in high-grade rocks. Gondwana Res 10:66–76

Passchier CW, Trouw RAJ (2005) Microtectonics. Springer, Heidelberg

Ramsay JG (1980) Shear zone geometry: a review. J Struct Geol 2:83–99

Ramsay JG, Lisle R (2000) The techniques of modern structural geology. Applications of continuum mechanics in structural geology, vol 3. Academic Press, San Francisco

Regenauer-Lieb K, Yuen DA (2003) Modeling shear zones in geological and planetary sciences: solid-and fluid-thermal-mechanical approaches. Earth-Sci Rev 63:295–349

Schlichting H, Gersten K (1999) Boundary layer theory, 8th edn. Springer, Berlin

Simpson C, De Paor DG (1993) Strain and kinematic analysis in general shear zones. J Struct Geol 15:1–20

Stüwe K (2007) Geodynamics of the lithosphere, 2nd edn. Springer, Berlin, p 325

Tejchman J (2008) Shear localization in granular bodies with micropolar hypoplasticity. Springer, Berlin. pp 24

Williams J, Elder SA (1989) Fluid physics for oceanographers and physicists: an introduction to incompressible flow. Pergamon Press, Oxford, pp 253–255

Xypolias P, Doutsos T (2000) Kinematics of rock flow in a crustal-scale shear zone: implication for the orogenic evolution of the southwestern Hellenides. Geol Mag 137:81–96

Xypolias P, Kokkalas S (2006) Heterogeneous ductile deformation along a mid-crustal extruding shear zone: an example from the External Hellenides (Greece). In: Law RD, Searle MP (eds) Channel flow, extrusion and exhumation in continental collision zones. Geol Soc Lond 268:497–516 (Spec Publ)